

# Graphical Abstract

## Estimating groundwater use and demand in arid Kenya through assimilation of satellite data and in-situ sensors with machine learning toward drought early action

Katie Fankhauser, Denis Macharia, Jeremy Coyle, Styvers Kathuni, Amy McNally, Kimberly Slinski, Evan Thomas

### DRIP Groundwater Use

**Year**  
2021

**County**  
All

**Measurement**  
Multiple Use Water Service (MUS) [1] (35+ L/pc/day)

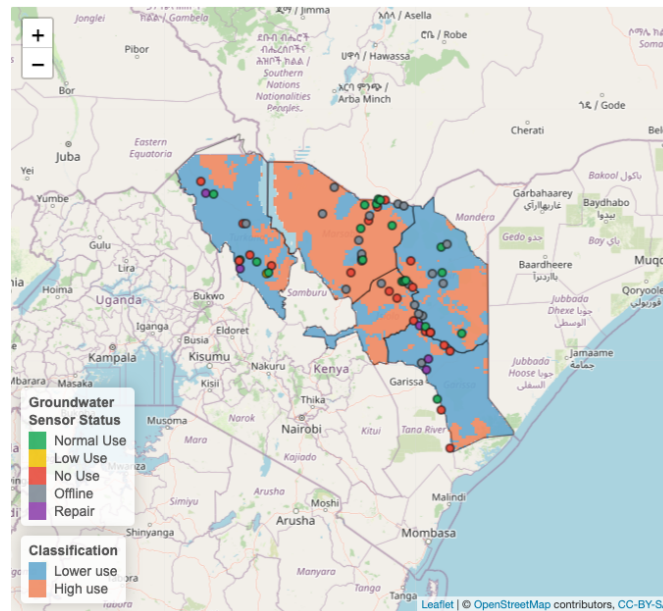
**Prediction**  
Classification of high use

**Display**  
Magnitude

Show current sensor status [2]  
 Show projected food security [3]

**Month**  
Jun 2021

[Return to Summary](#)



Expected accuracy: 74%

[1] <https://www.musgroup.net/>  
[2] <https://sweetsensors.com/>  
[3] <https://fewes.net/>

## Highlights

### **Estimating groundwater use and demand in arid Kenya through assimilation of satellite data and in-situ sensors with machine learning toward drought early action**

Katie Fankhauser, Denis Macharia, Jeremy Coyle, Styvers Kathuni, Amy McNally, Kimberly Slinski, Evan Thomas

- Supporting local groundwater management would improve resilience to drought.
- Kenya groundwater use estimated with sensors, satellite data, and machine learning.
- Historical use was modeled with up to 75% cross-validated accuracy.
- Forecasts for the 2021 dry season indicated up to 80% external validation accuracy.

# Estimating groundwater use and demand in arid Kenya through assimilation of satellite data and in-situ sensors with machine learning toward drought early action

Katie Fankhauser<sup>a</sup>, Denis Macharia<sup>a,b,c</sup>, Jeremy Coyle<sup>a,d</sup>, Styvers Kathuni<sup>d</sup>, Amy McNally<sup>e,f,g</sup>, Kimberly Slinski<sup>e,h</sup>, Evan Thomas<sup>a,d,\*</sup>

<sup>a</sup>*Mortenson Center in Global Engineering, University of Colorado Boulder, 4001 Discovery Drive, Boulder, 80303, Colorado, USA*

<sup>b</sup>*Regional Centre for Mapping of Resources for Development, Nairobi, Kenya*

<sup>c</sup>*Colorado, USA*

<sup>d</sup>*SweetSense Inc., USA*

<sup>e</sup>*NASA Goddard Space Flight Center, Greenbelt, Maryland, USA*

<sup>f</sup>*Science Applications International Corporation, Reston, Virginia, USA*

<sup>g</sup>*US Agency for International Development, Washington, DC, USA*

<sup>h</sup>*University of Maryland Earth Systems Science Interdisciplinary Center, College Park, Maryland, USA*

---

\*Corresponding author

*Email address:* `evan.thomas@colorado.edu` (Evan Thomas)

---

## Abstract

Groundwater is an important source of water for people, livestock, and agriculture during drought in the Horn of Africa. In this work, areas of high groundwater use and demand in drought-prone Kenya were identified and forecasted prior to the dry season. Estimates of groundwater use were extended from a sentinel network of 69 in-situ sensed mechanical boreholes to the region with satellite data and a machine learning model. The sensors contributed 756 site-month observations from June 2017 to September 2021 for model building and validation at a density of approximately one sensor per  $3,700 \text{ km}^2$ . An ensemble of 19 parameterized algorithms was informed by features including satellite-derived precipitation, surface water availability, vegetation indices, hydrologic land surface modeling, and site characteristics to dichotomize high groundwater pump utilization. Three operational definitions of high demand on groundwater infrastructure were considered: 1) mechanical runtime of pumps greater than a quarter of a day (6+ hrs) and daily per capita volume extractions indicative of 2) domestic water needs (35+ L), and 3) intermediate needs including livestock (75+ L). Gridded interpolation of localized groundwater use and demand was provided from 2017 to 2020 and forecasted for the 2021 dry season, June - September 2021. Cross-validated skill for contemporary estimates of daily pump runtime and daily volume extraction to meet domestic and intermediate water needs was 68%, 69%, and 75%, respectively. Forecasts were externally validated with an accuracy of at least 56%, 70%, 72% for each groundwater use definition. The groundwater maps are accessible to stakeholders including the Kenya National Drought Management Authority (NDMA) and the Famine Early Warning Systems Network (FEWS NET). These maps represent the first operational spatially-explicit sub-seasonal to seasonal (S2S) estimates of groundwater use and demand in the literature. Knowledge of historical and forecasted groundwater use is anticipated to improve decision-making and resource allocation for a range of early warning early action applications.

*Keywords:* drought, groundwater, early warning, early action, machine learning, remote sensing, Kenya

---

## 1. Introduction

Drought is one of the most persistent, expansive, and damaging of natural disasters. Coupled with weak institutional and civil systems, experience of drought leads to regional food insecurity, water insecurity, disease, and violent conflict for

5 billions of people globally (Wilhite and Glantz, 1985). The Horn of Africa is sus-  
6 ceptible to natural exposure and societal vulnerability to drought (Liebmann et al.,  
7 2017; NDMA, 2015). As a slow onset disaster, public and private organizations may  
8 not effectively mobilize resources in response (Cabot Venton, 2018). An advantage,  
9 however, is that the risk of drought can be monitored and forecasted in advance,  
10 allowing for the implementation of early warning early action systems (Funk and  
11 Shukla, 2020).

12 Drought early warning is an established field with existing indices that rely  
13 on climatological and land surface modeling or observing causal factors. For ex-  
14 ample, the United States National Integrated Drought Information System (NI-  
15 DIS) [drought.gov] produces current condition and 3-month drought outlooks from  
16 weather and climate, soil moisture, streamflow, and rainfall and snowpack data in-  
17 formed by qualitative expert opinion. In lower resource settings, such as Sub-Saharan  
18 Africa, observational data is sparse and satellite-derived and land surface modeled  
19 estimates of climate and the hydrologic cycle become the main inputs in drought  
20 monitoring. The Famine Early Warning Systems Network (FEWS NET) [few.net]  
21 makes the link between drought and food insecurity in low- and middle-income coun-  
22 tries explicit.

23 Drought develops from a deficit of precipitation and water storage inadequate  
24 to support livelihoods. The four domains of drought – meteorological, hydrological,  
25 agricultural, and socioeconomic – compound from an initial lack of rainfall and low-  
26 ered water availability to adverse impacts on land productivity and livestock and,  
27 ultimately, to water and food insecurity from diminished household returns (Wilhite  
28 and Glantz, 1985). The primary rainfall and agricultural season in East Africa has  
29 seen a marked decrease in precipitation in recent decades (Nicholson et al., 2018),  
30 leading to slower and lower recharge of surface water and diminished flow rates in  
31 large rivers. Moreover, the increase in surface temperatures from climate change,  
32 generates higher evapotranspiration, aggravating the decline in precipitation and  
33 intensifying aridification.

34 The arid and semi-arid lands (ASALs) of Kenya have faced regular drought since  
35 at least 2016 with below average rainfall placing 18 million people at risk (UNICEF,  
36 2017; KNBS, 2019). During times of low precipitation and decreased surface water  
37 capacity, groundwater becomes a critical source of water for domestic, livestock, and  
38 agricultural needs (Thomas et al., 2019). Pastoralist communities, in particular, are  
39 dependent on predictable access to water, without which they are likely to continue to  
40 experience inequitable rates of poverty and poor health (NDMA, 2015). Functional  
41 and strategic groundwater distribution, then, may lower exposure and vulnerability  
42 to drought for affected populations.

43 For the region, a number of databases are available that address water supply  
44 (Hofste et al., 2019; Senay et al., 2013) and demand (Hofste et al., 2019; McNally  
45 et al., 2019; Senay et al., 2015). Although these data products often incorporate  
46 some information about groundwater, they rely on Gravity Recovery and Climate  
47 Experiment (GRACE) satellite data at low resolution (10000 km<sup>2</sup> - 150000 km<sup>2</sup>)  
48 (Landerer and Swenson, 2012) or mechanistic hydrological modeling without other  
49 primary data. AQUASTAT (FAO, 2021) is a rich resource of water data, but it  
50 is only aggregated from annual questionnaires in tabulated form by country every 5  
51 years, limiting its usability at finer spatial scales and its relevance to real- or near-time  
52 response. Therefore, a geospatially explicit dataset that gives estimates of local (<50  
53 square kilometers) and acute (sub-seasonal) realized groundwater demand represents  
54 an important missing indicator of water resource availability and withdrawal that  
55 would improve interpretation of other water and drought indices in the region.

56 The Drought Resilience Impact Platform (DRIP) combines early detection with  
57 proactive groundwater management to ensure water availability with various stake-  
58 holders and decision support tools (Thomas et al., 2021). A principal feature of  
59 the platform is remote monitoring of a sentinel network of mechanical groundwa-  
60 ter boreholes in drought-prone regions of East Africa. The sensors have been used  
61 to identify non-functionality (Thomas et al., 2021), improve water service delivery  
62 and increase water infrastructure uptime (Nagel et al., 2015; Wilson et al., 2017),  
63 demonstrate an inverse relationship between rainfall and borehole use (Thomas et al.,  
64 2019), and examine a framework of groundwater management for drought resilience  
65 (Turman-Bryant et al., 2019). The current study explicitly addresses how monitoring  
66 data from the sensors can be used to quantify groundwater and improve delivery of  
67 drought early warning services and actions for the entire region.

68 Although groundwater is an essential water source, especially during the dry sea-  
69 son, during the 2016-2017 drought, 55% of the pumps needed to access groundwater  
70 were non-functional in Kenya (UNICEF, 2017). The ability to direct limited re-  
71 sources to repair, maintain, or site the most critically needed boreholes based on pro-  
72 jected use prior to drought would enable responsible stewardship of water resources  
73 and community resilience to drought. Interpreting use within known limitations of  
74 existing infrastructure may also help direct water resources other than groundwater,  
75 such as emergency water trucking. Furthermore, observing and predicting trends in  
76 groundwater use could be an important indicator of developing drought itself.

77 By leveraging additional remote sensing and in-situ data sources, we developed  
78 gridded estimates for historical and forecasted groundwater use in five prominent  
79 ASAL counties in Kenya. A statistical machine learning model extrapolates recorded  
80 borehole operation to locations that are not instrumented. The final product catego-

81 rizes areas into high vs. low groundwater use based on definitions of pump runtime  
82 and per capita volume extraction. This paper describes development of the DRIP  
83 groundwater service and presents the first gridded maps of acute groundwater use  
84 and demand in this context. It is expected to inform ongoing local management and  
85 planning for water and food insecurity during drought in Kenya and demonstrate  
86 this for East Africa.

## 87 **2. Methods**

### 88 *2.1. Context*

89 This work builds upon efforts of the Kenya Resilient Arid Lands Partnership  
90 for Integrated Development (Kenya RAPID) program. In-situ data was collected at  
91 all mechanized groundwater pumps identified as critical drought infrastructure and  
92 localized groundwater estimates were developed for five ASAL counties: Garissa,  
93 Isiolo, Marsabit, Turkana, and Wajir (Figure 1). Collectively the five counties cover  
94 approximately 260,000 square kilometers - or nearly half of the total surface area of  
95 Kenya - and suffer from water and food insecurity, high poverty rates, and limited  
96 access to basic services (NDMA, 2015). Despite several moderate to high produc-  
97 tivity sedimentary aquifers underlying the area, only 17% of renewable groundwater  
98 resources are being utilized (Mumma et al., 2011). The ASALs are expected to ex-  
99 perience more frequent and greater duration dry periods, likely exacerbating existing  
100 disadvantage in the absence of sustainable development and dedicated drought risk  
101 reduction.

102 The Government of Kenya has committed to ending drought emergencies (EDE)  
103 by 2022. The National Drought Management Authority (NDMA), established in  
104 2011, was directed to address drought proactively by confronting vulnerability and  
105 structural causes (NDMA, 2015). Cooperation between local county water officials  
106 and NDMA officials led to the selection of strategic boreholes for drought response  
107 that obtain financial and operational support. These boreholes in the five program-  
108 matic counties received sensor installation and monitoring. Previously, we observed  
109 that the strategic boreholes were more likely to be non-functional and susceptible to  
110 demand elasticity (Turman-Bryant et al., 2019). Drought triggers the mobilization  
111 of financial and material resources for maintenance of NDMA priority boreholes and  
112 the execution of contingency plans. In years where precipitation is higher, national  
113 and local resources for assessing drought risk and repair are withheld or reallocated,  
114 leading to an increase in the number and duration of malfunctions. The capacity  
115 to use strategic boreholes to mitigate future droughts is diminished by a smaller  
116 inventory of operating sites and increasing strain on remaining infrastructure. This

117 suggests that resources should consistently be directed to critical boreholes and to  
118 areas with restricted surface water availability or where demonstrable demand is  
119 already high.

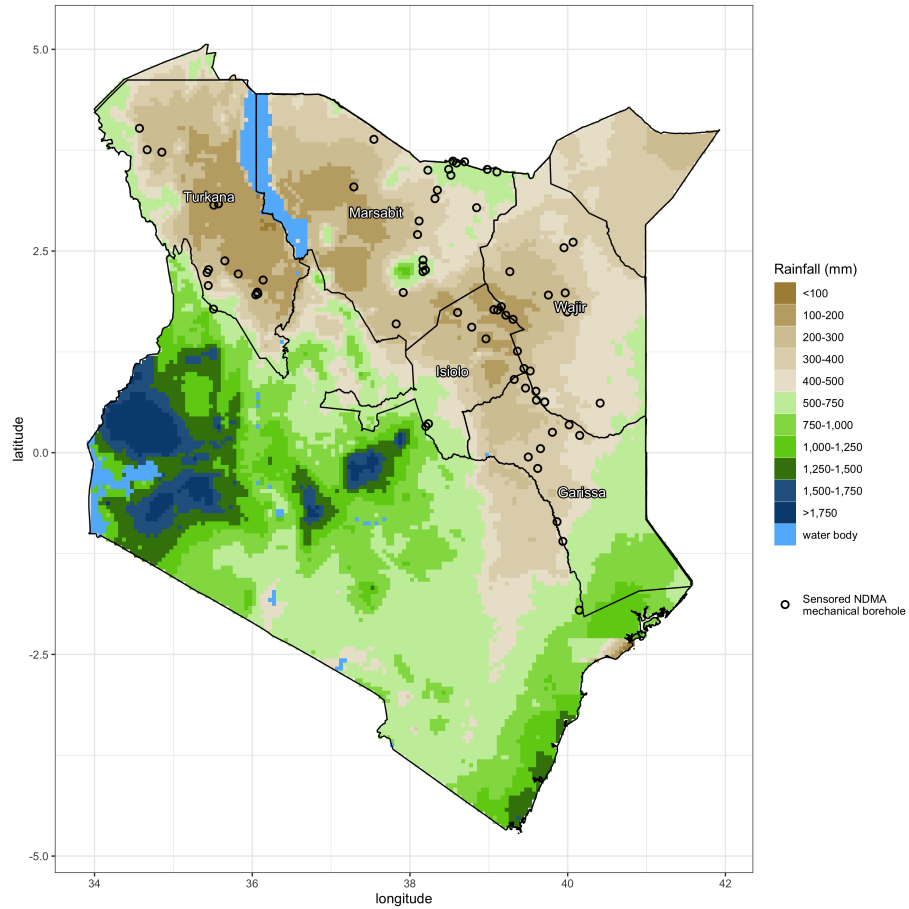


Figure 1: Average annual precipitation, 1981 - 2019. The locations of sensor-monitored NDMA (National Drought Management Authority) strategic drought emergency boreholes are shown in the five programmatic arid and semi-arid counties of Kenya. Data source: Climate Hazards Group InfraRed Precipitation with Station data (CHIRPS) v2.0

120 *2.2. Data*

121 *2.2.1. In-situ data*

122 From 2016 to present, 238 mechanized groundwater pumps in Kenya have been  
123 monitored by satellite- and cellular-connected sensors provided by SweetSense Inc.



124 (sweetsense.space). Pressac brand wireless current transformers measure the fre-  
125 quency and duration of borehole use by logging the electrical current (amperage)  
126 delivered to the mechanical pump over time. Data is transmitted daily to a central  
127 database and web application (Thomas et al., 2021). Sub-hourly sensor data was  
128 aggregated to mean daily pump runtime and volume by month.

129 NDMA selected the EDE strategic boreholes to prioritize for operations during  
130 drought. Further, data was subset to months during Kenya’s main dry season each  
131 year – June through September – as the annual period when drought is of biggest con-  
132 cern and deliberately surveilled. In-situ measurements from representative NDMA  
133 EDE boreholes were included in the sample when the mechanical borehole and sensor  
134 were reasonably known to be operational. Borehole and sensor status were assessed  
135 from maintenance surveys and the availability of daily data.

136 The final sample included 69 unique mechanical borehole sites (Figure 1) and 565  
137 site-month observations from June 2017 to September 2020. The four months of the  
138 2021 dry season (June - September 2021) contributed 191 site-month observations  
139 from 51 unique sites for external validation.

140 In order to provide comprehensive mapping of groundwater resources for differ-  
141 ent stakeholders and applications, three separate, but complementary, binary high  
142 groundwater use classifications were made from the sensor data. Each specification  
143 informs an aspect of groundwater accessibility, including physical infrastructure and  
144 population-based need. They are applied to the project region to be considered  
145 singularly or in comparison.

146 The three definitions of categorical high groundwater use by month translated  
147 from the sensor data are: 1) mean daily pump runtime over six hours per day (a  
148 quarter day) and mean daily per capita volume extracted 2) over 35 liters per person  
149 per day (L/pc/d) and 3) over 75 liters per person per day (L/pc/d). From the  
150 electrical current delivered to the pump, the number of hours a pump was switched on  
151 per day was measured and taken as pump runtime (Thomas et al., 2021). Estimated  
152 flow rate at the pump in cubic meters per hour was collected during site visits,  
153 and taking the product of runtime and yield provided estimates of volume of water  
154 extracted per day.

155 The high use threshold for pump runtime was set at approximately the observed  
156 mean while high per capita volume of over 35 L/pc/d was meant to capture basic  
157 needs on the multiple-use water services (MUS) ladder. Between 20 and 50 L/pc/d,  
158 users are expected to be able to meet most domestic and some livestock and per-  
159 sonal agricultural needs (MUS Group, 2013). Additionally, a threshold of over 75  
160 L/pc/d was considered to capture the higher water demands of pastoralists with  
161 livestock and represent an intermediate service level on the MUS ladder. Thus, lo-

162 cations of groundwater use at or above the high runtime or high volume thresholds  
163 indicate, respectively, areas where boreholes are expected to run longer than average  
164 or the population is relying on groundwater to meet domestic and livestock needs,  
165 presumably because other water resources are unavailable.

### 166 *2.2.2. Remote sensing data*

167 The variables taken or derived from satellite data were elevation (RCMRD Geo-  
168 portal, 2015); precipitation (Funk et al., 2015); surface water availability (Senay  
169 et al., 2013); baseflow, runoff, soil moisture, and actual evapotranspiration (Case  
170 et al., 2014); Normalized Difference Vegetation Index [NDVI] (USGS FEWS NET  
171 Data Portal, 2017); greenness vegetation fraction [GVF] (Vargas et al., 2015); and  
172 population density (Stevens et al., 2015). More detail about the actual nature of the  
173 features is given below in section 2.4.

174 Data was retrieved from January 2016 to May 2021 to cover the period of sensor-  
175 recorded observations of borehole use and accommodate lagging of time-varying co-  
176 variates for forecasting. Different temporal resolutions were ultimately averaged or  
177 summed by month. Native spatial resolution of the satellite data products ranged  
178 from 250 m to 50 km, and values were extracted at point coordinates of the sensors or  
179 centroids of a  $0.05^\circ \times 0.05^\circ$  ( $\sim 30 \text{ km}^2$ ) grid over the five counties. Higher resolution  
180 data were resampled using bilinear interpolation to agree with the reference grid.

181 Gridded population data at 1 km resolution was retrieved from WorldPop [worldpop.  
182 org] (Stevens et al., 2015; Lloyd et al., 2019) to scale sensor-derived groundwater vol-  
183 ume extraction by local population numbers. Volume per capita has been accepted  
184 as a proxy for water demand in previous studies (McNally et al., 2019).

### 185 *2.3. Supervised machine learning*

186 Supervised machine learning (ML) models are empirical. They optimize model  
187 fit to achieve the most similar outcomes to input training data without regard to  
188 deterministic or mechanistic explanations. Predictions are derived from the fit ap-  
189 plied to new observations. Ensemble ML (also known as Super Learning or model  
190 stacking) executes multiple models ("learners") on the same data and selects the  
191 optimal combination of them through cross-validation (van der Laan et al., 2007).  
192 Our library consisted of 19 candidate learners: nine XGBoost algorithms with dif-  
193 ferent hyperparameter selections (Chen and Guestrin, 2016); logistic regression; a  
194 Bayesian generalized linear model (Gelman et al., 2008); Ridge regression, LASSO  
195 regression, and another elastic net regularization with an alpha parameter equal to  
196 0.5 (Friedman et al., 2010); three k-Nearest Neighbors learners (Mouselimis, 2021)  
197 considering varying numbers of neighbors; Random Forests (Breiman, 2001); and a  
198 null model.

199 Covariates, or features, are the independent variables that have an assumed im-  
200 pact on the outcome (see section 2.4). Given the inclusion of algorithms in the  
201 ensemble that perform feature selection in addition to a pre-screening procedure,  
202 a large number of features, including those that are correlated, can be considered  
203 without overfitting the model. Overfitting occurs when a model describes training  
204 data well, but cannot generalize to new data. Feature selection and pre-screening  
205 reduce the number of features to improve parsimony and cross-validation retains in-  
206 dependence between training and testing datasets so that the model can predict new  
207 observations of groundwater use with accuracy. Furthermore, ensemble models are  
208 proven to perform as well as or better than any one candidate learner in the ensemble  
209 and minimizing cross-validated risk controls for overfitting even when a large number  
210 of learners are considered (van der Laan et al., 2007; Polley and Laan, 2010).

211 The purpose of modeling in this study was twofold: to extend runtime and volume  
212 predictions spatially and forward in time. To provide predictions across the region at  
213 a resolution of approximately 30 km<sup>2</sup>, a model trained and validated at instrumented  
214 boreholes was fit on independent explanatory features observed at centroid point  
215 coordinates of a 0.05° x 0.05° grid over the five programmatic counties. To extend  
216 the predictions forward in time, forecasting up to four months was achieved by  
217 lagging the features by the same number of months and individual model runs.  
218 Since the effect of climatological phenomenon on groundwater supply and demand  
219 may be delayed itself, we provided the model with all lagged features available at  
220 the respective forecast period and allowed the machine learner to screen and select  
221 the best performing lag for each time varying feature separately. For each outcome,  
222 the corresponding final model yielded a predicted probability that a certain centroid  
223 during a particular month was in a high use category as defined above. To establish  
224 binary high vs. low use, a threshold probability was selected based on a trade-off  
225 between true positive (high use borehole confirmed by the sensor record) and true  
226 negative (low use borehole confirmed by the sensor record) rates (see section 2.5).

227 To replicate operational conditions for the groundwater use forecasts and evaluate  
228 performance, we constrained model building between 2017 and 2020 and projected  
229 groundwater use forward for the 2021 dry season, June through September. Re-  
230 viewing anticipated groundwater use alongside current infrastructure functionality  
231 prior to the dry season should inform investments and actions taken by local water  
232 officers and national decision-makers to reduce drought risk. Moreover, we evaluated  
233 the skill of our forecasts, which serve as a source of external validation for future  
234 estimates.

235 Modeling and feature design of contemporary groundwater estimates respected an  
236 internal five-fold stratified cross-validation structure. In cross-validation the observed

237 data is sequentially partitioned into independent training and testing subsets. Five  
238 equally sized subsamples were generated randomly with all time series observations  
239 from one sensor being grouped in the same partition. The model was trained with  
240 four of the subsets and tested on the remaining, held-out subsample. This was  
241 repeated a total of five times (“folds”) with each of the subsamples being used once  
242 as the testing dataset. Cross-validation allows for the calculation of performance  
243 statistics and the ability to generalize the model to new data.

244 All data management and analysis was conducted in R statistical computing  
245 software (R Core Team, 2020).

#### 246 *2.4. Features*

247 The following variables are conventionally expected to influence drought and wa-  
248 ter insecurity and were included in our study: precipitation, land surface tempera-  
249 ture, vegetation indices, soil moisture profile, evapotranspiration, other hydrologic  
250 system dynamics such as baseflow and runoff, population density, geographic location  
251 (longitude, latitude, and elevation), and seasonality (Funk and Shukla, 2020).

252 The Climate Hazards Group InfraRed Precipitation with Station (CHIRPS) v2.0  
253 (Funk et al., 2015) is a 30+ year quasi-global rainfall dataset that incorporates satel-  
254 lite imagery with available in-situ station data to create  $0.05^\circ \times 0.05^\circ$  gridded rainfall  
255 time series. However, station data is inconsistent and inadequate over Africa. The  
256 Trans-African Hydro-Meteorological Observatory [TAHMO] (tahmo.org) is gradually  
257 enhancing weather data collection with the installation of low-cost stations across  
258 the continent (Giesen et al., 2014). Currently, they operate over 500 stations in 25  
259 countries, including 130 stations in Kenya. To leverage the advantages of both pre-  
260 cipitation datasets — the coverage and legacy of CHIRPS with the fine resolution  
261 in-situ data of TAHMO — we used inverse distance weighting (IDW) to interpo-  
262 late station data and combined the output with the satellite estimates at monthly  
263 time-scale through a Simple Bias Adjustment (SBA) merging method. The inter-  
264 polation was done using a maximum correlation distance of 250 km, achieving a  
265 minimum and maximum number of stations within this distance of two and ten,  
266 respectively. If there were no stations in the vicinity to correct the satellite estimate,  
267 the underlying CHIRPS grid value was retained, resulting in a spatially consistent  
268 bias-corrected gridded product. We adopted this method from the ENACTS merging  
269 process (Dinku et al., 2014).

270 Gridded maximum daily temperature from the Global Telecommunication System  
271 (GTS) of the World Meteorological Organization (WMO) was retrieved and averaged  
272 by month (Physical Sciences Laboratory). NDVI from the Collection 6 Moderate  
273 Resolution Imaging Spectroradiometer (MODIS) instrument on the Aqua satellite

274 was taken from processed data distributed by the United States Geological Survey  
275 (USGS) Earth Resources Observation and Science (EROS) Center (USGS FEWS  
276 NET Data Portal, 2017). GVF from the Visible Infrared Imaging Radiometer Suite  
277 (VIIRS) instrument aboard the Suomi National Polar-orbiting Partnership (NPP)  
278 and National Oceanic and Atmospheric Administration (NOAA)-20 satellites (Vargas  
279 et al., 2015) was based on the differences between the enhanced vegetation index  
280 (EVI) for bare soils and dense vegetation.

281 Land surface modeling (LSM) is a method to extend the coverage of hydrologic  
282 observations in data sparse contexts, such as remote and developing locations. The  
283 Noah-Multiparameterization (Noah-MP) LSM relies on water and energy balances  
284 to physically describe land-atmosphere interaction processes under multiple specifi-  
285 cations (Niu et al., 2011). Mean daily soil moisture ( $\text{m}^3/\text{m}^3$ ) at depths of 0 - 10 cm,  
286 10 - 40 cm, 40 - 100 cm, and 100 - 200 cm and total monthly actual evapotranspi-  
287 ration (mm), baseflow (mm), and runoff (mm) were derived from local instances of  
288 the Noah-MP LSM run per month (Case et al., 2014).

289 Population density was downloaded from WorldPop (worldpop.org) gridded pop-  
290 ulation data from combined geospatial and census data (Stevens et al., 2015; Lloyd  
291 et al., 2019). Data is provided only through 2020; for 2021, we applied a population  
292 growth rate of 2.3% to the 2020 data (The World Bank, 2021). Population den-  
293 sity was used as an independent variable when modeling pump runtime, but for per  
294 capita volume predictions, it was only used to scale the outcome and not as a model  
295 feature.

296 Other variables were included based on a demonstrable or logical relationship to  
297 groundwater use and demand. Public water management in Kenya is deregulated to  
298 the county level, leading to substantial differences in institutional and operational  
299 practices; thus, a county variable was added to describe unmeasured variability in  
300 groundwater supply and use due to administrative differences. Generally, deter-  
301 minants of the magnitude of groundwater use will be supply, demand, and access.  
302 Regionally interpolated relative surface water availability (Senay et al., 2013) was  
303 included to express the inverse correlation between rainfall, and by extension surface  
304 water supply, and borehole use (Thomas et al., 2019; Thomson et al., 2019). From  
305 a data inventory collated by Acacia Water as part of the Kenya RAPID program  
306 ([kenyarapid.acaciadata.com/map/13](http://kenyarapid.acaciadata.com/map/13)) we also considered the presence within 10 km  
307 of floodplains, lakes, springs, or river basins. Proximity to installed water infrastruc-  
308 ture, such as dams, sand pans, and other boreholes, may limit the use at any one  
309 groundwater source, and, therefore, counts of operational infrastructure within 10  
310 km were created. Calculated domestic water demand in 2015 provides an estimate  
311 of volume per square kilometer per day ( $\text{m}^3/\text{km}^2/\text{d}$ ) by sub-county required for ade-

312 quate human consumption (Tolk et al., 2016). Social and economic networks can be  
313 demonstrated by access to main roads, markets, or towns, or, in this case, a count  
314 of the number of these amenities within 10 km.

315 Livestock are one of the largest consumers of water in the ASALs. Pastoralists  
316 commonly direct their herds to boreholes along migration routes so the presence of  
317 a major livestock migration route within 10 km was added as a feature. Estimated  
318 water demand for livestock ( $\text{m}^3/\text{km}^2/\text{d}$ ) at the sub-county level was also included  
319 (Tolk et al., 2016).

320 We generated several variables from the sensor data to describe typical use behav-  
321 ior of boreholes in the region. One, we linearly regressed mean daily pump runtime or  
322 volume on static site characteristics, including longitude, latitude, elevation, county,  
323 water demand, proximity to natural water sources, other water infrastructure, and  
324 amenities, and livestock movement. Two, to leverage the sensor network and char-  
325 acterize the behavior of neighboring boreholes, we computed mean use at the five  
326 closest, by Euclidean distance, sensed sites as well as an interpolated layer of mean  
327 use at the maximally correlated site despite geographic location.

328 An advantage of using an ensemble learner and cross-validation is the ability to  
329 consider many features, models, and settings at once with less constraint on assuring  
330 a parsimonious model arising from a priori selection of the best set of variables and  
331 estimator (Polley and Laan, 2010). Thus, many social, environmental, and economic  
332 dimensions of drought risk and vulnerability were included. Ultimately, the ML  
333 was provided approximately 30 features from which each algorithm was built after  
334 screening.

335 See Appendix A for a detailed summary of all model features.

### 336 *2.5. Statistical Evaluation*

337 Model performance is evaluated by Receiver Operating Characteristic (ROC)  
338 curves and area under the curve (AUC), cross- and externally validated accuracy  
339 and rates of misclassification, and reliability diagrams. ROC curves are a perfor-  
340 mance measurement for classification problems. The ROC curve is a plot of sensi-  
341 tivity (y-axis) – the proportion of correctly identified instances of high use – against  
342 one minus specificity (x-axis) – the proportion of wrongly identified cases of high  
343 groundwater use among observed low use. The AUC demonstrates how good the  
344 model is at discriminating between high and low use. Determining which threshold  
345 to set when translating predicted probabilities to categories is always a trade-off be-  
346 tween sensitivity and specificity. Youden’s J statistic identifies the closest point on  
347 the ROC curve to the uppermost left corner of the plot and assumes both are equally  
348 important.

349 Accuracy is the percent number of sites where predicted high use correctly corre-  
350 sponds to observed high use after assigning predicted probabilities to above or below  
351 a set threshold. The null or no information rate (NIR) is the expected accuracy  
352 given random assignment based on the prevalence of the outcome in the data alone.  
353 Instances of incorrectly identified high use are evaluated with the false positive rate  
354 (FPR) and false negative rate (FNR) rate. The FPR is the proportion of wrongly  
355 identified cases of high groundwater use among observed low use. The FNR is relative  
356 to the number of misidentified low use among actual instances of high use.

357 Reliability is assessed from a linear relationship between predicted probability  
358 and observed frequency of high use relative to the magnitude of the probability. A  
359 perfectly reliable model exhibits a 1:1 relationship between the two.

### 360 **3. Results**

#### 361 *3.1. High resolution maps of groundwater use and demand*

362 The ensemble machine learning models allowed for the creation of high spatial  
363 and temporal resolution maps of groundwater use and demand. For each dry month  
364 June 2017 - September 2020 contemporary estimates of pump runtime and volume  
365 extracted at existing or hypothetical groundwater infrastructure are available at  
366 approximately 30 km<sup>2</sup> resolution. The most recent dry season, June - September  
367 2021, was forecasted and validated with ensuing observed data.

368 Figure 2 demonstrates how predicted probability output from the model was  
369 translated to high use for domestic needs ( $> 35$  L/pc/d). Red intensity indicates  
370 a higher probability of high use and ultimate high use class assignment is outlined.  
371 These maps may also suggest the certainty of high use classification. At a probability  
372 between 80-100%, we are relatively more confident groundwater use will surpass the  
373 high use threshold; if it is closer to 40-60%, we recognize that the model has identified  
374 one use category, but it may disagree with observed values on occasion.

375 Site-level accuracy for each 2021 month (72%, 74%, 77%, and 70%) showed that  
376 performance was relatively stable over different forecast periods, although it was  
377 lowest in September 2021 when the model had a lead of four months. High use  
378 was overestimated (i.e.,  $FPR > FNR$ ) in June and September and underestimated in  
379 July and August (i.e.,  $FNR > FPR$ ). When considering all years, specificity was high  
380 relative to sensitivity (Figure 4), indicating that generally the rate of false positives  
381 was lower than the rate of false negatives despite forecast lead time.

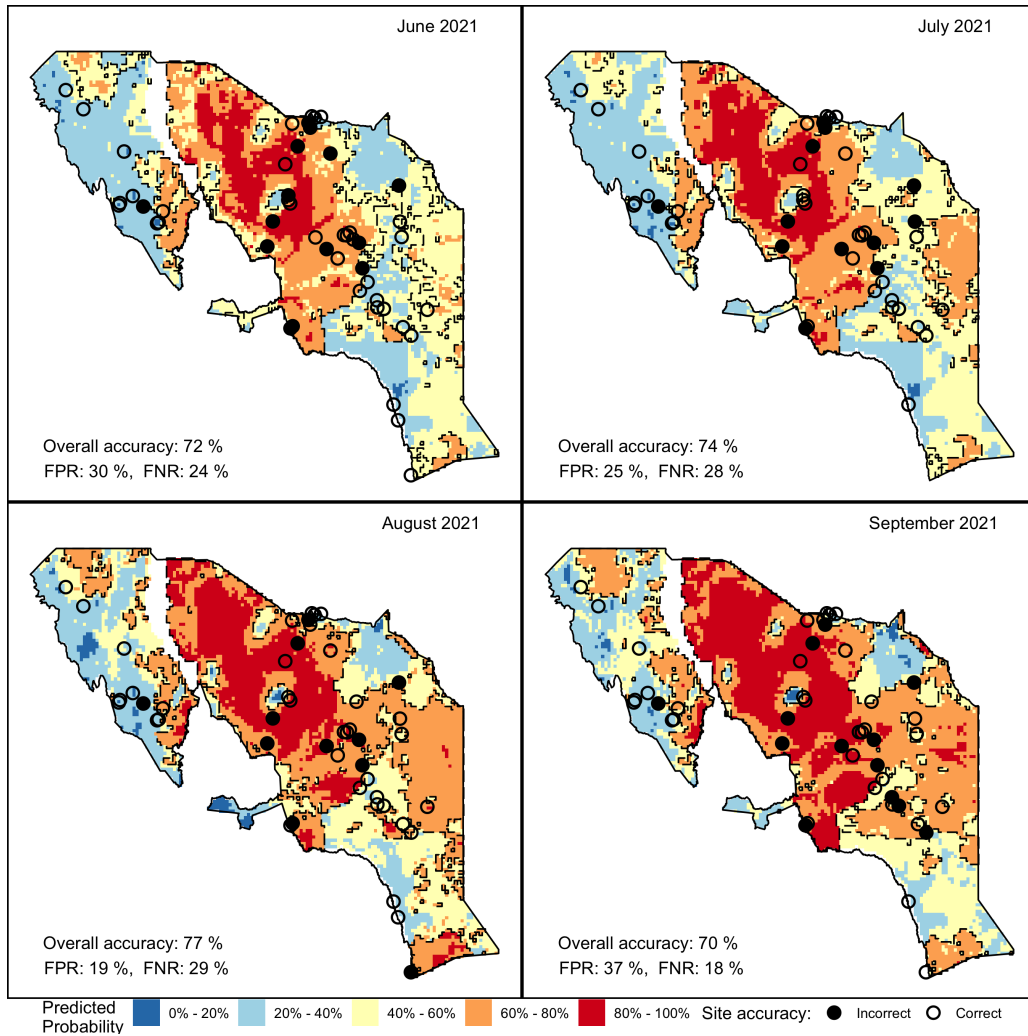


Figure 2: Predicted probability of groundwater demand for daily domestic water needs (>35 L per person per day) forecasted for the 2021 dry season. Categorization of high demand is outlined and accuracy is given for each dry season month. Rates of false positives (FPR) and false negatives (FNR) are based on site-level observations.

382 A similar demonstration was made for intermediate groundwater volume (> 75  
 383 L/pc/d) (Figure 3). Areas of northern Turkana County and southwestern Garissa  
 384 County showed diminished need for higher volumes indicative of livestock watering.  
 385 This was somewhat unexpected as these areas do support livestock. However, these  
 386 areas are also places of violent conflict. So while there may be a high need for water,  
 387 we anticipate some groundwater points in these region are demonstrating lower user



388 due to insecurity limiting access. There is unmet demand for water and rehabilitating  
389 water points or providing alternative water sources could serve to improve resource-  
390 based conflict in the area. Site accuracy was high (73-80%) and mis-identification of  
391 false negatives was more likely than false positives across the season.

392 Groundwater demand increased as the dry season progressed and was consistently  
393 highest in Marsabit and Isiolo counties for both domestic and livestock needs. Here  
394 only per capita volume was shown, but categories of pump runtime displayed similar  
395 patterns.

396 All maps are accessible via a web-based platform at [drip.shinyapps.io/groundwater](http://drip.shinyapps.io/groundwater).  
397 We presented only the pre-drought season 2021 volume per capita forecasts, but  
398 through the application, users can view historical and projected groundwater use.  
399 Other utilities include comparison of trends by month or year, viewing the two-class  
400 categorization of high groundwater use informed by the predicted probability, dis-  
401 playing the predictions as absolute magnitude or difference from averages, filtering  
402 by county, and seeing the status of the sensed boreholes.

403 For the purposes of this paper, we constrained model building prior to 2021 in  
404 order to externally validate the forecasts. In practice, the model and application will  
405 be updated per month during the dry season with an approximate one-week delay,  
406 at which time the concurrent groundwater estimates and forecasts roll forward one  
407 month. The model building procedure is repeated with the additional time series  
408 so the size and variability of the data will increase and we expect performance to  
409 improve over time with a longer data record.

### 410 *3.2. Performance of gridded contemporary and forecasted estimates*

411 The models achieved high statistical performance (Table 1, Figure 4). Estimation  
412 of volume per capita for domestic and intermediate needs proceeded the best.

413 The AUC for determining and forecasting high groundwater use ranged from  
414 0.703 to 0.714, from 0.746 to 0.756, and from 0.778 to 0.787 for daily pump runtime,  
415 domestic volume per capita, and intermediate volume per capita, respectively (Table  
416 1). Regardless if groundwater use is defined by mechanical requirements of the  
417 borehole or by water volume, our models contain a 70% or greater probability of  
418 accurately discriminating between low and high use. Ultimately, after classifying  
419 high use from predicted probabilities, the sensitivity for contemporary estimates, by  
420 use definition, was 58%, 57%, and 55% with corresponding specificity of 75%, 82%,  
421 and 88%. The rates for the one- to four-month forecasts were similar and can be  
422 read from Figure 4A. Since specificity is greater than sensitivity, it is less likely that  
423 a site predicted to exhibit high groundwater use would be incorrectly identified and  
424 there are less false positives than false negatives in the predictions. Thus, our models

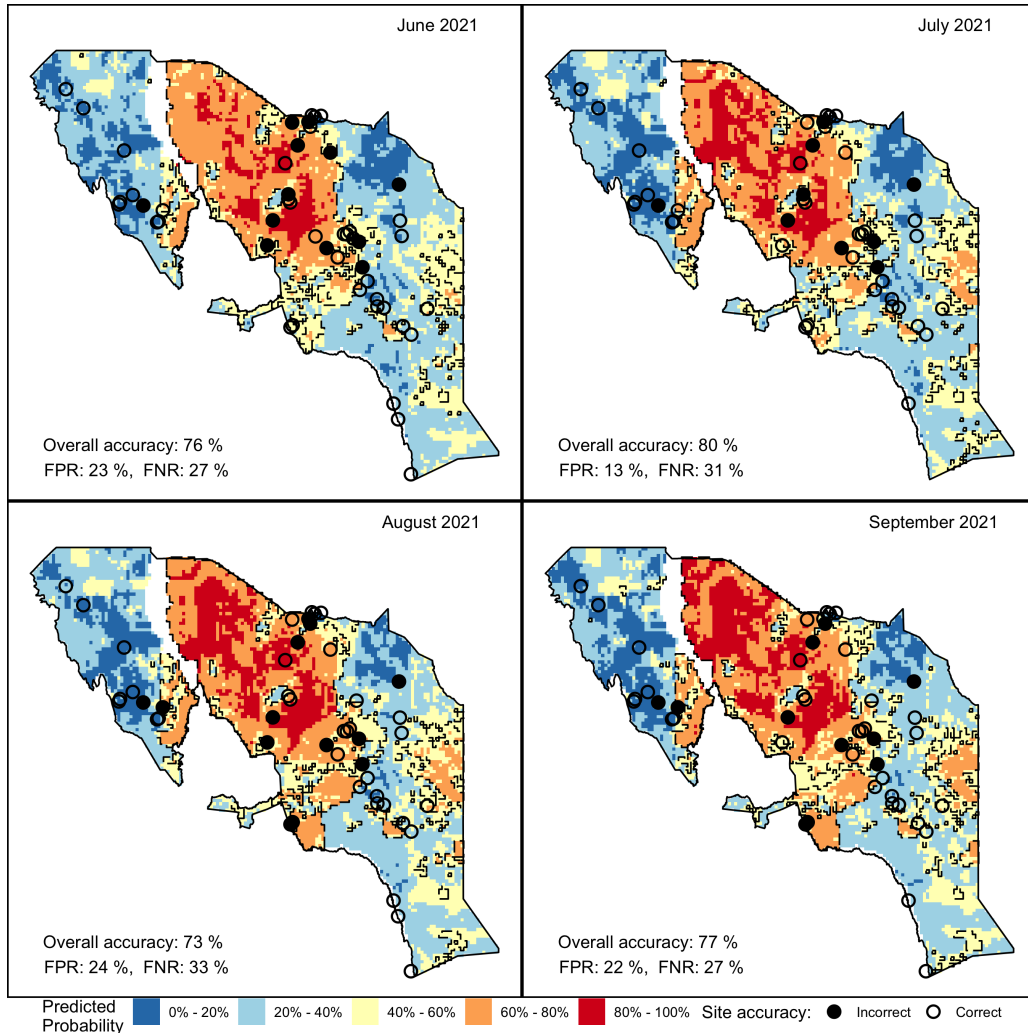


Figure 3: Predicted probability of groundwater demand for daily intermediate water needs (>75 L per person per day) forecasted for the 2021 dry season. Categorization of high demand is outlined and accuracy is given for each dry season month. Rates of false positives (FPR) and false negatives (FNR) are based on site-level observations.

425 are optimized to conserve material resources used to respond to high groundwater  
 426 need, such as deploying pump repair teams, at the occasional expense of failing to  
 427 capture some regions of high use.

428 Overall model accuracy (Table 1) of the contemporary categorical high runtime  
 429 and basic and intermediate volume per capita was 67.6%, 69.4%, and 74.5%, respec-  
 430 tively. A similar level of accuracy was observed for the one- to four-month forecasts.  
 431 High predictive skill of volume per capita was demonstrated with external validation,  
 432 indicating these models were not overfit. Accuracy was at least 70% and as high as  
 433 80% for forecasting per capita volume and represented significant improvement over  
 434 the NIR. Predictive skill of pump runtime was lower when tested on held-out data.

Table 1: Accuracy statistics for contemporary and one- to four-month forecasts of categorical high pump runtime (6+ hr/d), volume per capita for basic needs (35+ L/pc/d), and volume per capita for intermediate needs (75+ L/pc/d). Sensor data from the 2021 dry season was reserved from model building to provide evidence of operational accuracy for the forecasts from external validation. AUC = Area Under the Curve; NIR = No Information Rate; p-value = significance value of difference between accuracy and NIR

Model	AUC (95% CI)	Accuracy, % (p-value)	Validation Acc, %
Pump Runtime, 6+ hr/d	–	NIR: 57.7	–
Contemporary	0.705 (0.663 - 0.748)	67.6 (<0.001)	–
1 mo forecast - Jun 2021	0.706 (0.663 - 0.748)	66.5 (<0.001)	56.0
2 mo forecast - Jul 2021	0.714 (0.672 - 0.756)	66.9 (<0.001)	58.7
3 mo forecast - Aug 2021	0.703 (0.661 - 0.746)	63.9 (0.002)	56.2
4 mo forecast - Sep 2021	0.708 (0.666 - 0.750)	65.8 (<0.001)	57.4
Volume Per Capita, 35+ L/pc/d	–	NIR: 51.5	–
Contemporary	0.756 (0.717 - 0.796)	69.4 (<0.001)	–
1 mo forecast - Jun 2021	0.756 (0.717 - 0.795)	68.7 (<0.001)	72.0
2 mo forecast - Jul 2021	0.748 (0.708 - 0.787)	66.7 (<0.001)	73.9
3 mo forecast - Aug 2021	0.749 (0.709 - 0.788)	68.3 (<0.001)	77.1
4 mo forecast - Sep 2021	0.746 (0.705 - 0.786)	69.0 (<0.001)	70.2
Volume Per Capita, 75+ L/pc/d	–	NIR: 58.4	–
Contemporary	0.787 (0.749 - 0.825)	74.5 (<0.001)	–
1 mo forecast - Jun 2021	0.785 (0.747 - 0.823)	74.3 (<0.001)	76.0
2 mo forecast - Jul 2021	0.783 (0.745 - 0.821)	74.5 (<0.001)	80.4
3 mo forecast - Aug 2021	0.778 (0.739 - 0.817)	73.8 (<0.001)	72.9
4 mo forecast - Sep 2021	0.781 (0.742 - 0.820)	75.0 (<0.001)	76.6

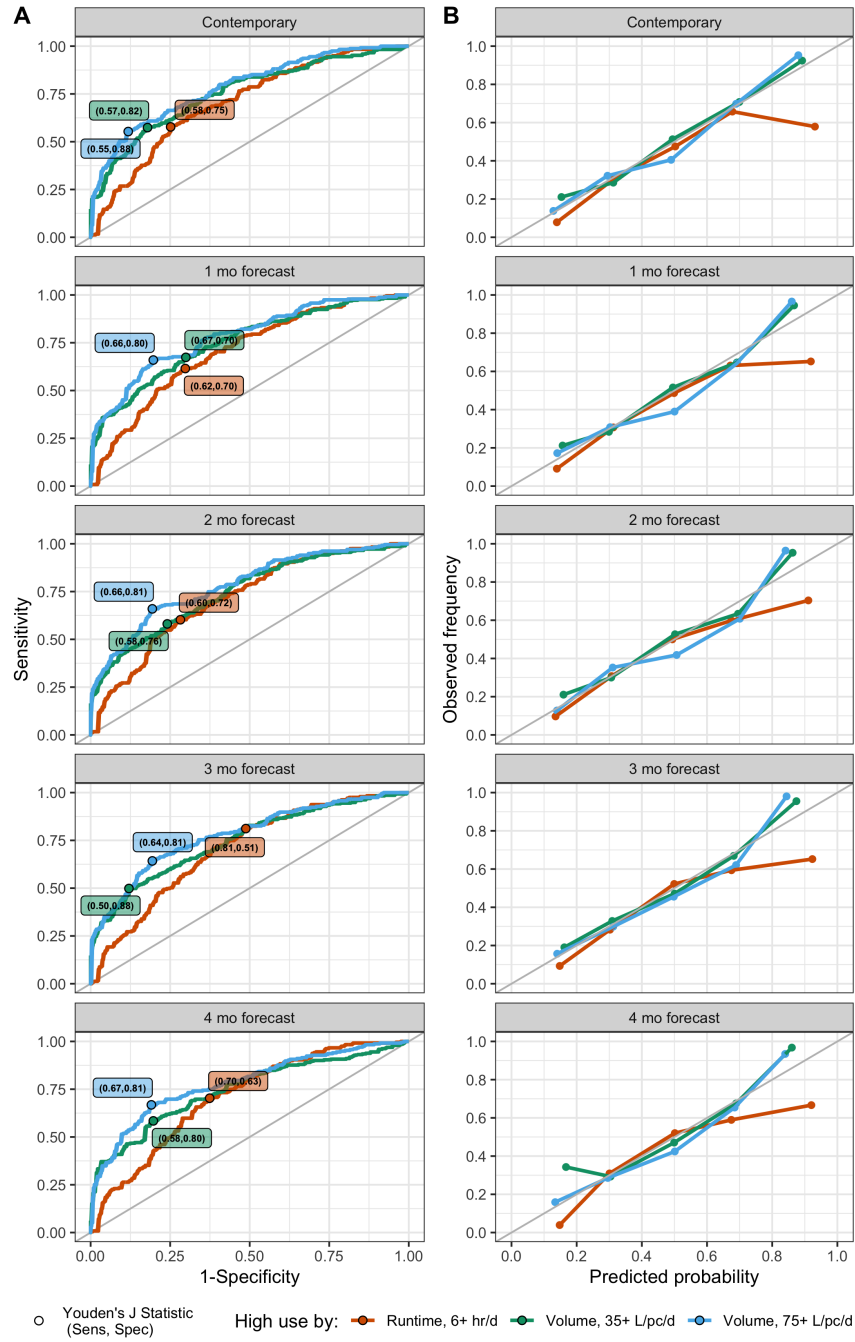


Figure 4: A) Receiver Operating Characteristic (ROC) curves and B) Reliability Diagrams. Performance given for pump runtime and volume per capita and by models used to estimate contemporary and forecasted groundwater use predictions.

435 Volume per capita predictions had the best reliability, exhibiting a consistent  
436 linear relationship between predicted probability and observed relative frequency  
437 (Figure 4B). Modeling of domestic volume per capita groundwater use assigned a  
438 probability of high use comparable to the occurrence of actual high use at each mag-  
439 nitude of probability except at the highest frequencies of use, when the probability  
440 was underestimated. At a lead time of four months, high use was also underestimated  
441 at the lowest frequencies of use. The model for groundwater use for intermediate  
442 water needs underestimated use at the highest frequencies and overestimated prob-  
443 ability at median frequencies. Prediction of pump runtime tended to overestimate  
444 the probability of high use.

### 445 *3.3. Contribution of model features*

446 Variable importance plots (Figure 5) indicate the relative information gained from  
447 the independent explanatory features. Variable importance is measured by the ratio  
448 in error, using negative log likelihood loss, between the full ensemble model and a  
449 model on modified data where the respective features have been excluded from model  
450 building. Features are plotted against the risk ratio, where model error without the  
451 features is divided by the error obtained from the full model. See Appendix A for  
452 which features are described by each theme. For example, in the one-month lagged  
453 models aimed at forecasting groundwater use in June 2021, removing administrative  
454 features (county, longitude, latitude, elevation, and proximity to towns, markets,  
455 and roads) increased model error by about 8% for pump runtime, between 4% and  
456 5% for basic per capita volume, and just over 1% for intermediate per capita vol-  
457 ume, indicating that, collectively, these variables were less informative for forecasting  
458 groundwater volume per capita needs.

459 The plots demonstrate patterns in what forces the groundwater use predictions  
460 for each use definition and lead time. In general, features related to typical, neigh-  
461 boring borehole behavior were not instructive of site usage. At a lag of one month,  
462 features related to or suggestive of water availability at the surface – such as pre-  
463 cipitation, water bodies, evapotranspiration, hydrology, and vegetation greenness –  
464 better informed volume per capita than pump runtime. With greater lagged obser-  
465 vations, i.e. as the hypothetical dry season progressed, the signal between features  
466 and per capita volume forecasts became less clear; although for pump runtime, many  
467 of the features shared a similar level of importance throughout. Models with longer  
468 lead (three and four months) demonstrated, with a risk ratio less than one, some fea-  
469 ture groups were damaging to model performance. This could be suggestive of some  
470 overfit or correlated variables within the group; however, since overall performance  
471 and accuracy of the forecasts were acceptable we did not investigate this further with

472 a systematic sensitivity analysis.

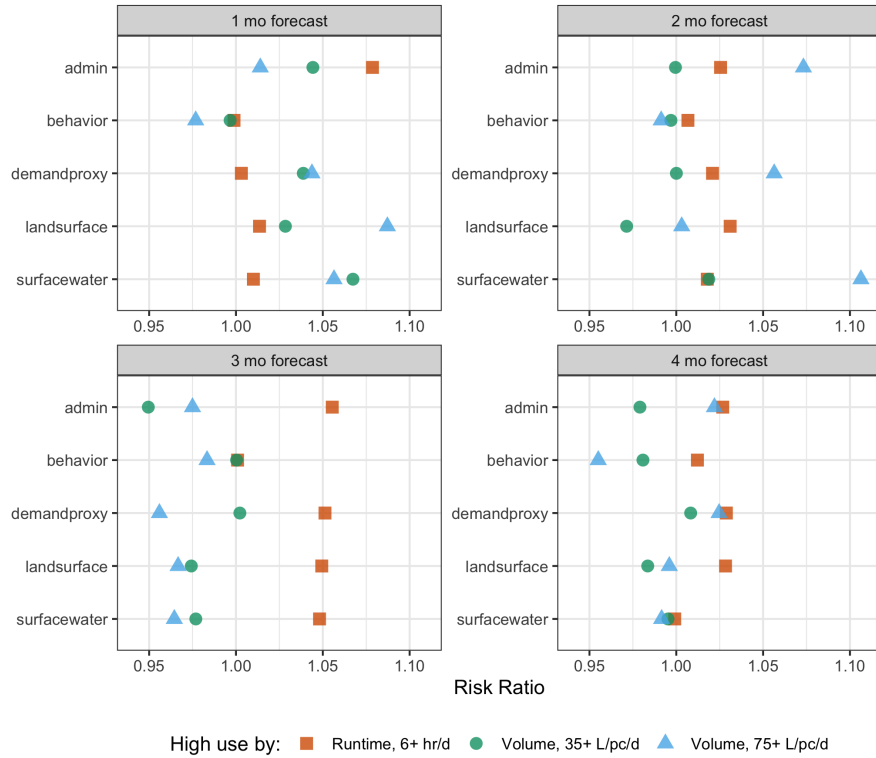


Figure 5: Variable importance plots for models predicting forecasted pump runtime and volume per capita. Covariates are grouped by theme; see Appendix A for which covariates are described by each theme.

#### 473 4. Discussion

474 These maps represent the first operational spatially-explicit sub-seasonal to sea-  
475 sonal (S2S) estimates of groundwater use and demand in the literature. The inte-  
476 gration of in-situ remote sensors with satellite data and hydrological land surface  
477 models through ensemble machine learning directly addresses an identified gap in  
478 population-based, near-real time, acute water monitoring (McNally et al., 2019) and  
479 supports other services for multi-dimensional drought early warning early action  
480 (Funk and Shukla, 2020).

481 The maps show areas of persistent high groundwater use, areas that develop a  
482 reliance on groundwater over the dry season, and locations where volume extraction  
483 suggests the requirement of groundwater to meet domestic needs for households and

484 watering of livestock for pastoralists. Previous work (Thomas et al., 2019) has iden-  
485 tified that pastoral and agropastoral households typically use a mix of groundwater  
486 and surface water to meet their needs, but have increased reliance on groundwater  
487 during dry seasons or in times of drought. Surface water or rainwater harvesting  
488 are preferred sources when available, with rural populations in Kenya reporting 34%  
489 less groundwater use during the wet season. The preference for surface water may  
490 be even more defined for livestock owners and the most water insecure populations  
491 (Thomson et al., 2019). Empirically we also observed an increase in borehole runtime  
492 and volume extraction during drought declared years and as the dry season advanced  
493 within years (see Section 4.1 below).

494 The ability to discriminate between high and low groundwater use did not atten-  
495 uate over the dry season despite lead time up to four months between predictions and  
496 predictive features. Groundwater needs become more acute as the dry season pro-  
497 gresses, resulting in a stronger measurable signal. Increasingly, rains prior to the dry  
498 season provide temporary relief, but are insufficient to provide adequate soil mois-  
499 ture for vegetation and recharge of surface water for the duration of the dry season.  
500 Thus, characterizing the hydrologic productivity of the rainy season, which occurs  
501 one to four months in advance, can explain patterns in subsequent groundwater use.

502 With external validation, forecasts of pump runtime proved to be non-informative  
503 during the 2021 dry season. Thus, there is likely additional unexplained variability  
504 among sites and activities supported by boreholes. Previous inventories of mechanical  
505 groundwater infrastructure in this region indicate that there are substantial differ-  
506 ences in withdrawal efficiencies due to size, manufacturer and operator, age, power  
507 source, and on-site storage (Thomas et al., 2019). Therefore, despite the introduc-  
508 tion of an additional source of error when translating mechanical pump runtime to  
509 volume with a yield coefficient, predictive skill of volume per capita was highest,  
510 particularly for intermediate ( $> 75$  L/pc/d) use. Instead, we believe that flowrate  
511 helped control for differences in pump capacity and implementation. Moreover, a  
512 higher volume threshold likely further differentiated between boreholes used for crit-  
513 ical drought mitigation during the dry season specifically and other EDE-targeted  
514 boreholes that might have been used more indiscriminately.

515 Predictors related to surface water availability – satellite and gauged precipita-  
516 tion, relative depth of freshwater water points, and proximity to other natural water  
517 bodies – were indicative of volume per capita model performance at one and two  
518 month lead times. Many of the other satellite-derived and modeled hydrological  
519 features had an inconsistent effect on model error. The change in relative variable  
520 importance by forecast lead time highlights that characterizing water resources and  
521 drought dynamically and 'on-the-ground' with respect to human behavior is complex.

522 The utility of a statistically driven model is the assimilation of satellite data, land  
523 surface models, and field data into accurate estimates that lead to actionable insights  
524 in the absence of a clear or complete deterministic understanding. This is especially  
525 relevant to Sub-Saharan Africa, a context of sparse monitoring data, limited capac-  
526 ity, and developing scientific consensus of the agro-hydrological mechanisms driving  
527 drought (Funk and Shukla, 2020).

#### 528 *4.1. Estimated impact of groundwater demand on drought risk and planning*

529 The methodology presented here could not have proceeded without in-situ data,  
530 but we have demonstrated that low density sensors can integrate satellite data and  
531 mechanistic land surface modeling for local groundwater monitoring. The fine spatial  
532 and temporal resolution of our gridded groundwater use and demand maps has not  
533 been achievable before. Approximately 70 sensors were used to inform a total area of  
534  $260,000 \text{ km}^2$ , or one sensor per  $3,700 \text{ km}^2$  ( $1,500 \text{ mi}^2$ ). A small network of sentinel  
535 sensors provides economical and efficient means to ground-truth and expand the  
536 utility of earth observation data.

537 We made a pixel-to-point comparison between the gridded groundwater estimates  
538 and observed site data. One-to-one comparisons between gridded satellite data and  
539 station observations have been practiced in the literature (Dinku et al., 2014) and  
540 while they have been shown to represent area averages less well than pixel-to-pixel  
541 comparisons (Dinku et al., 2018), the method is relevant to our context. In the  
542 ASALs of northern Kenya residents may walk up to 10 km to collect water for  
543 domestic needs and pastoralists walk even greater distances in search of livestock  
544 watering. Generating estimates at  $0.05^\circ \times 0.05^\circ$ , roughly equal to  $5 \text{ km} \times 5 \text{ km}$ ,  
545 is appropriate for describing water collection behavior then. Additionally, the use  
546 of high vs. low categories smooths differences in groundwater use attributable to  
547 unexplained site variability at this scale. We report high cross-validated accuracy at  
548 this density and resolution. Thus, the modeled groundwater use/demand pixels did  
549 characterize site-level observations well.

550 The distribution of sensors in the five program counties was not uniform, but  
551 this was by design with respect to drought emergency. NDMA and county officials  
552 identified strategic EDE boreholes for monitoring and water resource managers an-  
553 ticipate areas without sensors to be lower priority during drought response because  
554 of low population densities, uninterrupted water resources other than groundwater,  
555 or other mitigating factors. Despite these differences, similar hydrological, climato-  
556 logical, and socioeconomic conditions are captured at sensed sites since the ASALs  
557 share many common characteristics (NDMA, 2015). In counties with better distribu-  
558 tion of sensors, such as Turkana, predictions were accurate across a range of different



559 conditions. Moreover, in areas of predicted high use without existing EDE prior-  
 560 ity, our predictions may prompt re-evaluation of EDE resources and mobilization of  
 561 additional in-situ data collection.

562 Gridded groundwater demand contains essential information for decision-makers  
 563 in settings experiencing or expecting drought. The percent area and percent of pop-  
 564 ulation affected by reliance on groundwater each year can be enumerated from our  
 565 maps (Table 2). We delineated trends in groundwater use over time that can be  
 566 related to other meteorological and hydrological phenomenon. The national govern-  
 567 ment of Kenya declared drought in 2017 after several years of low precipitation. An  
 568 above-average long rains season in 2018 helped sustain improvements in water and  
 569 food security, but the next year saw a return to drier conditions and higher tempera-  
 570 tures and, subsequently, 2019 was another year of drought. However, rainfall toward  
 571 the end of the year and during the 2020 long rains promoted recovery. Unfortunately,  
 572 the following two rainy seasons were critically below average, and another national  
 573 drought disaster was declared in 2021 (OCHA, 2021a). The ASALs, where now over  
 574 2.5 million people are facing water and food shortages, have been especially impacted  
 575 (OCHA, 2021b). We see relative changes reflected in high groundwater demand dur-  
 576 ing drought years and accurately forecasted higher demand prior to the 2021 dry  
 577 season (Table 2).

Table 2: Frequency of predicted high groundwater use over northern Kenya by percent of total area and population affected each year at any point during the dry season (June - September) of that year. Population counts were taken from WorldPop unconstrained UN Census adjusted estimates (Lloyd et al., 2019).

Year	Pump Runtime		Volume Per Capita		Volume Per Capita	
	6+ hr/d		35+ L/pc/d		75+ L/pc/d	
	Area (%)	Popl (%)	Area (%)	Popl (%)	Area (%)	Popl (%)
2017	54.2	50.3	64.3	40.4	33.6	10.1
2018	46.5	40.6	59.8	30.1	40.3	12.9
2019	51.5	49.0	57.9	27.4	37.0	10.0
2020	49.6	43.6	57.6	28.1	40.4	11.7
2021	71.4	68.4	63.1	34.7	45.0	14.7

578 A review of the 2021 dry season before it begins (Table 3), provided national and  
 579 county officials with the total and percent of their constituents expected to be living  
 580 under circumstances contributing to high groundwater use, such as limited surface

581 water and lowered access to other services. Percent change in groundwater use by the  
 582 end of the dry season demonstrates how and where need changes. All counties were  
 583 expected to experience an increase (positive change) in groundwater reliance as the  
 584 dry season progressed with one exception. In Isiolo, the percent of the population  
 585 expected to undertake high groundwater use to meet basic water needs decreased  
 586 from June to September. Counties that experienced the greatest change, such as  
 587 Wajir and Garissa, may engender more attention and resource allocation for early  
 588 warning early action services.

Table 3: Impact of 2021 dry season. Total and percent of population predicted to experience high groundwater use at the start of the 2021 dry season (June) by county and the the percent increase in population expected to be relying on groundwater by the end of the dry season (September). Population counts were taken from WorldPop unconstrained UN Census adjusted estimates (Lloyd et al., 2019).

County	Pump Runtime			Volume Per Capita			Volume Per Capita		
	6+ hr/d			35+ L/pc/d			75+ L/pc/d		
	<i># thous.</i>	%	% chg	<i># thous.</i>	%	% chg	<i># thous.</i>	%	% chg
All	1830	35.9	63.4	1050	20.7	61.2	424	8.3	49.5
Garissa	392	24.1	45.5	123	7.6	140.5	34.1	2.1	81.9
Isiolo	72.7	39.5	14.3	105	57.0	-5.2	59.1	32.1	33.1
Marsabit	179	49.2	40.0	202	55.8	10.0	187	51.4	9.1
Turkana	859	72.5	25.8	191	16.1	24.9	65.1	5.5	56.3
Wajir	326	18.8	207.7	432	24.9	94.8	78.5	4.5	138.0

589 Several actions are anticipated from these maps in advance of drought. When  
 590 mapped together, sensor data indicating pumps needing repair where high usage  
 591 is predicted would be an alert to prioritize maintenance services to these monitored  
 592 sites. Where there are no sensors, this kind of assessment would need to proceed from  
 593 the institutional knowledge of local water officers, field scientists, and other experts.  
 594 Thus, if high usage is predicted in areas without adequate borehole coverage and/or  
 595 functionality — known through prior or external sources — then resources should  
 596 be devoted to new installations, maintenance, and other water infrastructure.

597 The models had a higher specificity than sensitivity, meaning there were fewer  
 598 false positive results and the risk of allocating resources to increase water availabil-  
 599 ity unnecessarily is lower. Conversely, this interpretation accepts that that some  
 600 instances of need will be missed. We chose a threshold to balance sensitivity and

601 specificity for the highest overall accuracy, but the two parameters can be changed  
602 based on programmatic priorities.

603 Operational drought monitoring for Sub-Saharan Africa has been relatively nascent  
604 in the last decade, when satellite data and land surface modeling were leveraged to  
605 establish historical climatology and forecast parameters related to meteorological,  
606 agricultural, and hydrological drought, such as precipitation, soil moisture, vege-  
607 tation, and streamflow. Yet, most monitors do not include a unique groundwater  
608 component.

609 FEWS NET provides several drought indicators (McNally et al., 2019), and ad-  
610 ditionally the water supply and demand product for crops, the Water Requirement  
611 Satisfaction Index (WRSI) (Senay et al., 2015), and surface water levels, the Wa-  
612 terpoint Viewer (Senay et al., 2013). Acute water stress monitoring related these to  
613 population needs (McNally et al., 2019). Although, given that these analyses are typ-  
614 ically generated from renewable freshwater resources and that the volume of stored  
615 groundwater is estimated to be 100 times that of annual renewable sources and 20  
616 times the volume of freshwater lakes in Africa, groundwater as a resource to meet  
617 domestic, pastoral, and agricultural needs is missing from water scarcity assessments  
618 (MacDonald et al., 2012). These datasets in large part form the evidence base of  
619 food security classifications and risk outlooks.

620 Thus, we propose the DRIP groundwater use and demand maps will become  
621 another reference dataset for drought indices and expand the knowledge base for  
622 decision making in Kenya and other future operational contexts. A challenge will  
623 be how to systematically integrate localized groundwater withdrawal estimates as  
624 a quantitative feature, but we have identified potential to apply them to drought  
625 monitoring through expert interpretation and guidance with several key stakeholders.

#### 626 *4.2. Case study applications*

627 Stakeholder consultations were a critical component of this research. We con-  
628 ducted regular consultations with scientists at the eastern and southern Africa SERVIR  
629 hub – the Regional Centre for Mapping of Resources for Mapping (RCMRD) – and  
630 FEWS NET in order to align the groundwater use and demand products with user  
631 needs. We also organized two user engagement workshops. The first workshop was  
632 held in February 2021 and was attended by drought management officers from the  
633 NDMA. The second meeting was held in June 2021 and focused on the rollout of pro-  
634 totype products for Marsabit County in Kenya. Participants in the second meeting  
635 were drawn from NDMA, the Kenya Meteorological Department, drought humani-  
636 tarian agencies including the Kenya Red Cross Society (KRCS), Mercy Corps, and  
637 Food for the Hungry, and the county departments of information technology and

638 water services.

639 We received three important recommendations from these meetings: (i) the need  
640 for participatory planning and co-development of community early warning systems  
641 that leverage groundwater use and demand information from DRIP, (ii) continuous  
642 improvement of the groundwater use and demand products through expert feedback  
643 and user-based validations, and (iii) linking the products to existing drought infor-  
644 mation dissemination mechanisms through the NDMA national and county drought  
645 bulletins. These recommendations are part of future co-development processes. The  
646 development of the groundwater products is also synergistic with other rangeland  
647 vegetation monitoring services by RCMRD and national drought early warning early  
648 actions program led by the KRCS.

#### 649 *4.2.1. The Famine Early Warning System Network (FEWS NET)*

650 FEWS NET scientists and domain experts (co-authors McNally and Slinski),  
651 reviewed the DRIP groundwater platform for its potential to inform the FEWS  
652 NET analysis of acute food insecurity risk. The risk of acute food insecurity is a  
653 function of a particular hazard or shock, the vulnerability of a specific population,  
654 and that population's ability to cope, or recover, from the shock. This framework  
655 informs the FEWS NET scenario development process that allows for the projection  
656 of food insecurity eight months in advance for humanitarian assistance planning.

657 The ASALs of Kenya are subject to shocks that include drought, animal pests  
658 and diseases, limited access to dry season grazing, and cattle raiding. Some com-  
659 munities additionally experience inadequate access to water for domestic use and  
660 watering livestock, especially during the dry season. This results in the occurrence  
661 of waterborne disease and poor animal health which are additional shocks to the sys-  
662 tem. Much of the population in northern Kenya relies on livestock for food and cash  
663 income (FEWS NET, 2011). Thus, given the nature of the hazards and vulnerability  
664 of the livestock sector, the ability of this region to cope tends to be low. In late 2021,  
665 this region was experiencing Phase III - Crisis food insecurity which is characterized  
666 by households that either have above usual acute malnutrition or are marginally able  
667 to meet minimum food needs by depleting essential assets or engaging in negative  
668 coping strategies.

669 The predictions of groundwater use and demand can be helpful to the FEWS  
670 NET scenario development process. As previously mentioned, groundwater demand  
671 is indicative of inadequate access to water from other sources, like surface water and  
672 shallow water infrastructure due either to non-functionality or drought. In this way,  
673 groundwater demand forecasts could alert food security analysis of a shift in behavior  
674 toward using available groundwater. In many locations, however, the groundwater

675 maps and overlaid in-situ sensor data show that households have inadequate access  
676 to groundwater during crucial periods (e.g., dry season) due to non-functionality of  
677 infrastructure at nearby boreholes.

678 This unmet need, which contributes to the risk of food insecurity, could be high-  
679 lighted in FEWS NET reporting and in turn addressed by decision-makers (e.g.  
680 programmers of humanitarian assistance or national water ministries) in a number  
681 of different ways: 1) encouraging water point rehabilitation, including repair and  
682 maintenance of pumps, in locations where DRIP indicates that wells are not prop-  
683 erly functioning; 2) alternative solutions like water trucking could be employed in  
684 locations where wells do not exist or are unable to be repaired; 3) institutionalization  
685 of reliable access to groundwater through installation of new boreholes and increased  
686 support of pump maintenance in longer term planning documents. Preventive action  
687 to ensure sustainable groundwater access may be particularly useful in locations that  
688 suffer from unreliable water trucking due to inaccessibility or political factors.

689 Prior to the 2021 dry season and before the current drought in Kenya became  
690 apparent, our forecasts would have indicated an increased demand in groundwater  
691 relative to 2020 (Table 2). An increased reliance on groundwater in times of drought  
692 may, in some cases, involve traveling long distances to Kenya’s EDE strategic bore-  
693 holes. These predictions were consistent with the observed situation in the September  
694 2021 Key Message Update (FEWS NET, 2021): “an atypically high number of live-  
695 stock are migrating to dry season grazing areas driven by the decline in rangeland  
696 and water resources. Between July and August, livestock trekking distances to wa-  
697 tering points increased by 60-90 percent, likely driving the 13-55 percent decline in  
698 milk production compared to the three-year average. [...] Overall, the decline in  
699 livestock productivity and body conditions is constraining household access to food  
700 and income and maintaining area-level Crisis (IPC Phase 3) outcomes across pastoral  
701 areas.”

702 Taken together, knowledge of groundwater demand and FEWS NET risk profiles  
703 could have initiated concrete early actions such as borehole rehabilitation and pump  
704 repair or alternative reliable access to water through, for example, water trucking to  
705 improve water and food security during this year’s drought.

#### 706 *4.2.2. The Kenya National Drought Management Authority (NDMA)*

707 NDMA exercises coordination across drought risk management and establishes  
708 mechanisms, either on its own or with stakeholders, that will end drought emergencies  
709 in Kenya (NDMA, 2015). NDMA has headquarter offices in Nairobi, Kenya and has  
710 established sub-offices in 23 arid and semi-arid counties considered vulnerable to  
711 drought. County Steering Groups (CSG) manage the coordination of drought and

712 early warning information at the county level in Kenya (USAID, 2018). The CSG  
713 is co-chaired by the county governor and county commissioner while the NDMA is  
714 the secretariat. Based on NDMA’s overall mandate and role in guiding the agenda  
715 and discussion at CSG meetings, they have been targeted as a critical user of data  
716 on groundwater.

717 From predicted groundwater demand, NDMA and other stakeholders can identify  
718 mitigation activities against the effects of drought, such as identifying areas  
719 with predicted high water demand whose borehole pumps would require preventive  
720 maintenance. The Ministry of Water at the county would conduct timely budgeting,  
721 procurement of spare parts, and plan visits by borehole technicians to specific sites.  
722 Further, by analyzing the predicted water demand in relation to production capacities  
723 of boreholes in an area, NDMA and stakeholders could advise communities on  
724 migration that is usually triggered by the search for water. Such timely advice has  
725 the potential to avert violence between communities over competition of resources  
726 that has been common during the drought period. Thus, knowledge of groundwater  
727 patterns and forecasts helps public agencies address multi-dimensional impacts of  
728 drought, including health, livelihoods, and conflict.

#### 729 *4.3. Limitations and Future Work*

730 In northern Kenya, groundwater supply is not a limiting factor. Recharge and  
731 fossil quantities in aquifers are higher than abstraction rates and are capable of  
732 providing groundwater (Mumma et al., 2011). This assumption would need to be  
733 revisited when applying this framework in new settings. Instead, being able to extract  
734 groundwater from functional infrastructure is a limitation that may contribute to  
735 unmet demand for water and under or overestimate use in our maps. We know  
736 from sensor reports and the motivation behind the DRIP theory of change (Thomas  
737 et al., 2020) that mechanical boreholes in this region are, in fact, often non-functional.  
738 In this study, our data filters attempted to remove the most persistent periods of  
739 non-functionality, and we have begun to identify and correct for functional status  
740 (Thomas et al., 2021). Our maps represent areas where dependence on groundwater  
741 at strategically located boreholes is high under the assumption that EDE boreholes  
742 do exist and are functioning in that area; if neither of these assumptions prove to be  
743 valid, that in and of itself may be the justification to initiate a response.

744 The inclusion of forecasted climatology as model features, to supplement or sup-  
745 plant the current lagged observations, should be explored. Predicting the dry season  
746 from conditions at a one to four month lead was demonstrated here because hydro-  
747 logical and agricultural drought, and subsequent reliance on groundwater, should be  
748 strongly correlated to conditions during the long rains season, March through May

749 (Shukla et al., 2021). However, incorporation of other forecasted drought indicators,  
750 which are often built from decades of historical climatology, could improve our pre-  
751 dictive ability during years outside the range of values observed since in-situ borehole  
752 monitoring.

753 Further development of the gridded groundwater maps and DRIP service will  
754 focus on application and amplifying the wider context of groundwater health and  
755 potential for agricultural and rangeland productivity. Installation of groundwater  
756 level sensors and modeling of trends in groundwater level will address aquifer health,  
757 local overdraft, and sustainability of groundwater use. As groundwater is promoted  
758 and leveraged as a drought mitigation strategy, appropriate development and man-  
759 agement supported by monitoring will be critical.

## 760 **5. Conclusion**

761 Groundwater represents an opportunity to increase reliable water supplies in  
762 Africa and provide a buffer against drought. Improving accessibility to groundwater  
763 through better maintenance of water systems and responsible development of new  
764 water schemes are mitigation strategies that reduce drought risk and improve re-  
765 siliience. Sustainable, effective, and local management of groundwater resources and  
766 infrastructure is a necessary precondition to achieving water security, as is accurate  
767 monitoring of changing water needs in a changing climate. The Drought Resilience  
768 Impact Platform fine resolution gridded dry season groundwater use and demand  
769 maps are a novel data source that can be used directly to allocate resources as well  
770 as provide a groundwater component to other water and food insecurity indices as  
771 part of multi-sectoral, multi-dimensional drought early warning and early action.

## 772 **6. Funding**

773 The work described in this publication was made possible through support pro-  
774 vided by the National Aeronautics and Space Administration, under the terms of  
775 Grant No. 80NSSC20K0150; the National Science Foundation under the terms of  
776 Award No. 1738321; and the U.S. Agency for International Development, under the  
777 terms Cooperative Agreement No. AID-615-A-15-00008. The opinions expressed  
778 herein are those of the authors and do not necessarily reflect the views of the U.S.  
779 Agency for International Development.

780 **Appendix A. Characteristics of Data Features**

781 Features, or covariates, provided to groundwater prediction models. Theme relates to grouped features held out to test  
 782 variable importance; see Figure 5. Res is the data product’s native resolution. <sup>1</sup>Population density was used as an independent  
 783 variable in pump runtime models, but for per capita volume predictions it was only used to scale the outcome and not as a  
 784 model feature.

<b>Coded Name</b>	<b>Theme</b>	<b>Description</b>	<b>Units</b>	<b>Res</b>
amenities	admin	presence of major or primary roads, markets, or towns within 10 km	numeric (0 - 4)	–
county	admin	county	discrete (Turkana, Marsabit, Isiolo, Wajir, Garissa)	–
dem	admin	elevation from Digital Elevation Model	m	30 m
x	admin	longitude, east/west location	decimal degrees in WGS84	–
y	admin	latitude, north/south location	decimal degrees in WGS85	–
corrneighbor_*	behavior	average daily pump runtime or volume of interpolated 5 most linearly correlated sensed boreholes	hours or L/per capita	5 km
geoneighbor_*	behavior	average pump runtime or volume of 5 closest by Euclidean distance sensed boreholes	hours or L/per capita	–
geoneighbor_dist	behavior	distance between site or grid centroid and 5 closest sensed boreholes	km	–
proxy_*	behavior	modeled average daily pump runtime or volume based on static site characteristics	hours or L/per capita	–
boreholes_krapid	demandproxy	number of boreholes (inventory identified by Kenya RAPID) within 10 km	numeric	–
dams_or_pans	demandproxy	number of dams and sand pans (identified by Kenya RAPID) within 10 km	numeric	–
livestock_h2o	demandproxy	estimated amount of water required for livestock in 2015	discrete (>0.26, >0.50, >1.0, >1.5, >3.5 m <sup>3</sup> /km <sup>2</sup> /day)	subcounty
livestock_route	demandproxy	presence of major livestock migration route within 10 km	binary (0, 1)	–
month_factor	demandproxy	categorical month	discrete (1 - 12)	–



<b>Coded Name</b>	<b>Theme</b>	<b>Description</b>	<b>Units</b>	<b>Res</b>
people_h2o	demandproxy	estimated domestic water demand in 2015	discrete (>1030, >2000, >6000, m <sup>3</sup> /day)	subcounty >4000, >8000
popldens <sup>1</sup>	demandproxy	estimated population density, number of people per square kilometer	numeric	1 km
baseflow	landsurface	total baseflow, streamflow that is sustained between precipitation events	mm	3 km
et	landsurface	total actual evapotranspiration	mm	3 km
gvf	landsurface	greenness vegetation fraction	proportion (0 - 1)	4 km
maxtemp	landsurface	average daily maximum temperature	degrees Celsius	50 km
ndvi	landsurface	average 10-day maximum Normalized Difference Vegetation Index value	proportion (0 - 1)	250 m
runoff	landsurface	total amount of flow of water across the ground surface after it no longer infiltrates the soil	mm	3 km
soilm1	landsurface	average daily soil moisture in top layer at depths of 0 - 10 cm	m <sup>3</sup> /m <sup>3</sup>	3 km
soilm2	landsurface	average daily soil moisture at depths of 10 - 40 cm	m <sup>3</sup> /m <sup>3</sup>	3 km
soilm3	landsurface	average daily soil moisture at depths of 40 - 100 cm	m <sup>3</sup> /m <sup>3</sup>	3 km
soilm4	landsurface	average daily soil moisture at depths of 100 - 200 cm	m <sup>3</sup> /m <sup>3</sup>	3 km
chirps	surfacewater	total precipitation from Climate Hazards Group InfraRed Precipitation with Station (CHIRPS) v2.0	mm	5 km
naturalh2o	surfacewater	presence of floodplains, lakes, springs, or river basins with 10 km	numeric (0 - 4)	–
tahmo_chirps	surfacewater	total localized precipitation, CHIRPS v2.0 scaled and bias-corrected with Trans-African Hydro-Meteorological Observatory (TAHMO) weather stations	mm	5 km
waterpoint_depth	surfacewater	average daily interpolated relative surface water depth	percentage (0 - 100)	5 km

785 **References**

- 786 Breiman, L., 2001. Random Forests. *Machine Learning* 45, 5–32. doi:10.1023/A:  
787 1010933404324.
- 788 Cabot Venton, C., 2018. Economics of Resilience to Drought: Kenya Analysis.  
789 Technical Report. USAID Center for Resilience.
- 790 Case, J.L., LaFontaine, F.J., Bell, J.R., Jedlovec, G.J., Kumar, S.V., Peters-Lidard,  
791 C.D., 2014. A Real-Time MODIS Vegetation Product for Land Surface and Nu-  
792 merical Weather Prediction Models. *IEEE Transactions on Geoscience and Remote*  
793 *Sensing* 52, 1772–1786. doi:10.1109/TGRS.2013.2255059.
- 794 Chen, T., Guestrin, C., 2016. XGBoost: A Scalable Tree Boosting System, in:  
795 Proceedings of the 22nd ACM SIGKDD International Conference on Knowledge  
796 Discovery and Data Mining, Association for Computing Machinery, New York,  
797 NY, USA. pp. 785–794. doi:10.1145/2939672.2939785.
- 798 Dinku, T., Funk, C., Peterson, P., Maidment, R., Tadesse, T., Gadain, H., Ceccato,  
799 P., 2018. Validation of the CHIRPS satellite rainfall estimates over eastern Africa.  
800 *Quarterly Journal of the Royal Meteorological Society* 144, 292–312. doi:10.1002/  
801 qj.3244.
- 802 Dinku, T., Hailemariam, K., Maidment, R., Tarnavsky, E., Connor, S., 2014. Com-  
803 bined use of satellite estimates and rain gauge observations to generate high-quality  
804 historical rainfall time series over Ethiopia. *International Journal of Climatology*  
805 34, 2489–2504. doi:10.1002/joc.3855.
- 806 FAO, 2021. AQUASTAT. URL: <https://www.fao.org/aquastat/en/>.
- 807 FEWS NET, 2011. Livelihoods zoning "plus" activity in Kenya. Techni-  
808 cal Report. URL: [https://fews.net/sites/default/files/documents/reports/KE\\_](https://fews.net/sites/default/files/documents/reports/KE_livelihood_profiles.pdf)  
809 [livelihood\\_profiles.pdf](https://fews.net/sites/default/files/documents/reports/KE_livelihood_profiles.pdf).
- 810 FEWS NET, 2021. Consecutive below-average agricultural seasons in-  
811 crease household food insecurity. URL: [https://fews.net/east-africa/kenya/](https://fews.net/east-africa/kenya/key-message-update/september-2021)  
812 [key-message-update/september-2021](https://fews.net/east-africa/kenya/key-message-update/september-2021).
- 813 Friedman, J.H., Hastie, T., Tibshirani, R., 2010. Regularization Paths for Gener-  
814 alized Linear Models via Coordinate Descent. *Journal of Statistical Software* 33,  
815 1–22. doi:10.18637/jss.v033.i01.

- 816 Funk, C., Peterson, P., Landsfeld, M., Pedreros, D., Verdin, J., Shukla, S., Husak,  
817 G., Rowland, J., Harrison, L., Hoell, A., Michaelsen, J., 2015. The climate hazards  
818 infrared precipitation with stations—a new environmental record for monitoring  
819 extremes. *Scientific Data* 2. doi:10.1038/sdata.2015.66.
- 820 Funk, C., Shukla, S., 2020. *Drought Early Warning and Forecasting: Theory and*  
821 *Practice*. Elsevier Inc.
- 822 Gelman, A., Jakulin, A., Pittau, M.G., Su, Y.S., 2008. A weakly informative default  
823 prior distribution for logistic and other regression models. *The Annals of Applied*  
824 *Statistics* 2. doi:10.1214/08-AOAS191.
- 825 Giesen, N.v.d., Hut, R., Selker, J., 2014. The Trans-African Hydro-Meteorological  
826 Observatory (TAHMO). *WIREs Water* 1, 341–348. doi:10.1002/wat2.1034.
- 827 Hofste, R.W., Kuzma, S., Walker, S., Sutanudjaja, E.H., Bierkens, M.F.P.,  
828 Kuijper, M.J.M., Sanchez, M.F., Beek, R.V., Wada, Y., Rodríguez,  
829 S.G., Reig, P., 2019. *Aqueduct 3.0: Updated Decision-Relevant*  
830 *Global Water Risk Indicators* URL: [https://www.wri.org/research/](https://www.wri.org/research/aqueduct-30-updated-decision-relevant-global-water-risk-indicators)  
831 [aqueduct-30-updated-decision-relevant-global-water-risk-indicators](https://www.wri.org/research/aqueduct-30-updated-decision-relevant-global-water-risk-indicators).
- 832 KNBS, 2019. *Volume I: Population by County and Sub-County*. Technical Report.  
833 Kenya National Bureau of Statistics.
- 834 van der Laan, M.J., Polley, E.C., Hubbard, A.E., 2007. Super learner. *Statistical*  
835 *Applications in Genetics and Molecular Biology* 6. doi:10.2202/1544-6115.1309.
- 836 Landerer, F.W., Swenson, S.C., 2012. Accuracy of scaled GRACE terrestrial water  
837 storage estimates. *Water Resources Research* 48. doi:10.1029/2011WR011453.
- 838 Liebmann, B., Bladé, I., Funk, C., Allured, D., Quan, X.W., Hoerling, M., Hoell,  
839 A., Peterson, P., Thiaw, W.M., 2017. Climatology and Interannual Variability  
840 of Boreal Spring Wet Season Precipitation in the Eastern Horn of Africa and  
841 Implications for Its Recent Decline. *Journal of Climate* 30, 3867–3886. doi:10.  
842 1175/JCLI-D-16-0452.1.
- 843 Lloyd, C.T., Chamberlain, H., Kerr, D., Yetman, G., Pistolesi, L., Stevens, F.R.,  
844 Gaughan, A.E., Nieves, J.J., Hornby, G., MacManus, K., Sinha, P., Bondarenko,  
845 M., Sorichetta, A., Tatem, A.J., 2019. *Global spatio-temporally harmonised*  
846 *datasets for producing high-resolution gridded population distribution datasets*.  
847 *Big Earth Data* 3, 108–139. doi:10.1080/20964471.2019.1625151.

- 848 MacDonald, A.M., Bonsor, H.C., Dochartaigh, B., Taylor, R.G., 2012. Quantitative  
849 maps of groundwater resources in Africa 7. doi:10.1088/1748-9326/7/2/024009.
- 850 McNally, A., Verdin, K., Harrison, L., Getirana, A., Jacob, J., Shukla, S., Arsenault,  
851 K., Peters-Lidard, C., Verdin, J.P., 2019. Acute Water-Scarcity Monitoring for  
852 Africa. *Water* 11. doi:10.3390/w11101968.
- 853 Mouselimis, L., 2021. KernelKnn: Kernel k Nearest Neighbors. URL: [https://CRAN.  
854 R-project.org/package=KernelKnn](https://CRAN.R-project.org/package=KernelKnn).
- 855 Mumma, A., Lane, M., Kairu, E., Tuinhof, A., Hirji, R., 2011. Kenya Groundwater  
856 Governance Case Study. Technical Report. World Bank. Washington, DC. URL:  
857 <https://openknowledge.worldbank.org/handle/10986/17227>.
- 858 MUS Group, 2013. Briefing Note: Matching Water Services with Water Needs. Tech-  
859 nical Report. Multiple Use Water Services Group. URL: [https://www.musgroup.  
860 net/node/6](https://www.musgroup.net/node/6).
- 861 Nagel, C., Beach, J., Iribagiza, C., Thomas, E.A., 2015. Evaluating Cellular Instru-  
862 mentation on Rural Handpumps to Improve Service Delivery—A Longitudinal  
863 Study in Rural Rwanda. *Environmental Science & Technology* doi:10.1021/acs.  
864 est.5b04077.
- 865 NDMA, 2015. Common Programme Framework for Ending Drought Emer-  
866 gencies. Technical Report. National Drought Management Authority.  
867 Nairobi, Kenya. URL: [https://www.ndma.go.ke/index.php/resource-center/send/  
868 43-ending-drought-emergencies/4251-common-programme-framework](https://www.ndma.go.ke/index.php/resource-center/send/43-ending-drought-emergencies/4251-common-programme-framework).
- 869 Nicholson, S.E., Funk, C., Fink, A.H., 2018. Rainfall over the African continent from  
870 the 19th through the 21st century. *Global and Planetary Change* 165, 114–127.  
871 doi:10.1016/j.gloplacha.2017.12.014.
- 872 Niu, G.Y., Yang, Z.L., Mitchell, K.E., Chen, F., Ek, M.B., Barlage, M., Kumar, A.,  
873 Manning, K., Niyogi, D., Rosero, E., Tewari, M., Xia, Y., 2011. The community  
874 Noah land surface model with multiparameterization options (Noah-MP): 1. Model  
875 description and evaluation with local-scale measurements. *Journal of Geophysical  
876 Research: Atmospheres* 116. doi:10.1029/2010JD015139.
- 877 OCHA, 2021a. Kenya: Drought - 2014-2021. URL: [https://reliefweb.int/disaster/  
878 dr-2014-000131-ken](https://reliefweb.int/disaster/dr-2014-000131-ken).

879 OCHA, 2021b. Kenyan ASAL counties continue to face the  
880 brunt of the Drought. URL: [https://reliefweb.int/report/kenya/  
881 kenyan-asal-counties-continue-face-brunt-drought](https://reliefweb.int/report/kenya/kenyan-asal-counties-continue-face-brunt-drought).

882 Physical Sciences Laboratory, . CPC Global Daily Temperature. URL: [https://psl.  
883 noaa.gov/data/gridded/data.cpc.globaltemp.html](https://psl.noaa.gov/data/gridded/data.cpc.globaltemp.html).

884 Polley, E., Laan, M.v.d., 2010. Super Learner In Prediction. U.C. Berkeley Di-  
885 vision of Biostatistics Working Paper Series URL: [https://biostats.bepress.com/  
886 ucbbiostat/paper266](https://biostats.bepress.com/ucbbiostat/paper266).

887 R Core Team, 2020. R: A Language and Environment for Statistical Computing.  
888 R Foundation for Statistical Computing, Vienna, Austria. URL: [https://www.  
889 R-project.org/](https://www.R-project.org/).

890 RCMRD Geoportal, 2015. Kenya SRTM 30 Meters. URL: [http://geoportal.rcmr.  
891 org/layers/servir%3Akenya\\_srtm30meters](http://geoportal.rcmr.org/layers/servir%3Akenya_srtm30meters).

892 Senay, G., Velpuri, N., Bohms, S., Budde, M., Young, C., Rowland, J., Verdin,  
893 J., 2015. Drought Monitoring and Assessment, in: Hydro-Meteorological Hazards,  
894 Risks and Disasters. Elsevier, pp. 233–262. URL: [https://linkinghub.elsevier.com/  
895 retrieve/pii/B9780123948465000096](https://linkinghub.elsevier.com/retrieve/pii/B9780123948465000096).

896 Senay, G.B., Velpuri, N., Alemu, H., Md Pervez, S., Asante, K.O., Kariuki, G.,  
897 Taa, A., Angerer, J., 2013. Establishing an operational waterhole monitoring  
898 system using satellite data and hydrologic modelling: Application in the pastoral  
899 regions of East Africa. Pastoralism: Research, Policy and Practice 3. doi:10.  
900 1186/2041-7136-3-20.

901 Shukla, S., Husak, G., Turner, W., Davenport, F., Funk, C., Harrison, L., Krell, N.,  
902 2021. A slow rainy season onset is a reliable harbinger of drought in most food  
903 insecure regions in Sub-Saharan Africa. PLOS ONE 16. doi:10.1371/journal.  
904 pone.0242883.

905 Stevens, F.R., Gaughan, A.E., Linard, C., Tatem, A.J., 2015. Disaggregating Census  
906 Data for Population Mapping Using Random Forests with Remotely-Sensed and  
907 Ancillary Data. PLOS ONE 10. doi:10.1371/journal.pone.0107042.

908 The World Bank, 2021. Population growth (annual %) - Kenya. URL: [https://data.  
909 worldbank.org/indicator/SP.POP.GROW?locations=KE](https://data.worldbank.org/indicator/SP.POP.GROW?locations=KE).

- 910 Thomas, E., Wilson, D., Kathuni, S., Libey, A., Chintalapati, P., Coyle, J., 2021.  
911 A contribution to drought resilience in East Africa through groundwater pump  
912 monitoring informed by in-situ instrumentation, remote sensing and ensemble ma-  
913 chine learning. *Science of The Total Environment* 780. doi:10.1016/j.scitotenv.  
914 2021.146486.
- 915 Thomas, E.A., Kathuni, S., Wilson, D., Muragijimana, C., Sharpe, T., Kaberia, D.,  
916 Macharia, D., Kebede, A., Birhane, P., 2020. The Drought Resilience Impact Plat-  
917 form (DRIP): Improving Water Security Through Actionable Water Management  
918 Insights. *Frontiers in Climate* 2. doi:10.3389/fclim.2020.00006.
- 919 Thomas, E.A., Needoba, J., Kaberia, D., Butterworth, J., Adams, E.C., Oduor,  
920 P., Macharia, D., Mitheu, F., Mugo, R., Nagel, C., 2019. Quantifying increased  
921 groundwater demand from prolonged drought in the East African Rift Valley.  
922 *Science of The Total Environment* 666, 1265–1272. doi:10.1016/j.scitotenv.  
923 2019.02.206.
- 924 Thomson, P., Bradley, D., Katilu, A., Katuva, J., Lanzoni, M., Koehler, J., Hope,  
925 R., 2019. Rainfall and groundwater use in rural Kenya. *Science of The Total*  
926 *Environment* 649, 722–730. doi:10.1016/j.scitotenv.2018.08.330.
- 927 Tolk, L., de Vries, A., de Wildt, S., 2016. 3R/MUS Analysis: Data Inventory, Kenya  
928 RAPID. Technical Report. Acacia Water. URL: <https://kenyarapid.acaciadata.com/>.
- 930 Turman-Bryant, N., Nagel, C., Stover, L., Muragijimana, C., Thomas, E.A., 2019.  
931 Improved Drought Resilience Through Continuous Water Service Monitoring  
932 and Specialized Institutions—A Longitudinal Analysis of Water Service Deliv-  
933 ery Across Motorized Boreholes in Northern Kenya. *Sustainability* 11, 3046.  
934 doi:10.3390/su11113046.
- 935 UNICEF, 2017. Kenya Humanitarian Situation Report. Technical Report. United  
936 Nations Children’s Emergency Fund. URL: <https://reliefweb.int/report/kenya/unicef-kenya-humanitarian-situation-report-20-february-2017>.
- 938 USGS FEWS NET Data Portal, 2017. eMODIS AQUA Normalized Difference Veg-  
939 etation Index (NDVI). URL: <https://earlywarning.usgs.gov/fews/product/448>.
- 940 Vargas, M., Jiang, Z., Ding, H., NOAA JPSS Program Office, 2015. NOAA JPSS  
941 Visible Infrared Imaging Radiometer Suite (VIIRS) Green Vegetation Fraction  
942 (GVF) from NDE.

- 943 Wilhite, D.A., Glantz, M.H., 1985. Understanding the Drought Phenomenon: The  
944 Role of Definitions. *Water International* 10, 111–120.
- 945 Wilson, D.L., Coyle, J.R., Thomas, E.A., 2017. Ensemble machine learning and  
946 forecasting can achieve 99% uptime for rural handpumps. *PLOS ONE* 12. doi:10.  
947 1371/journal.pone.0188808.